

Current Concepts of Cross-Sectional and Functional Anatomy of the Cerebellum: A Pictorial Review and Atlas

Vance T Lehman MD, David F Black MD, David R DeLone MD, Daniel J Blezek
PhD, Timothy J Kaufmann MD, Waleed Brinjikji MD, and Kirk M Welker MD

Department of Radiology, Mayo Clinic, Rochester MN

Running head: Cerebellum: structural, functional and imaging review

Manuscript type: Pictorial review

Author for correspondence

Vance Lehman, MD

Department of Radiology

Mayo Clinic

200 First Street SW

Rochester MN 55905

Email: lehman.vance@mayo.edu

Phone: 507-266-1207

FAX: 507-266-1657

Conflicts of Interest: TJK: Consult for SpineThera and stock option ownership, not relevant to current work; all other authors have no conflicts of interest to declare.

Funding: The authors have no funding to declare.

Acknowledgements: The authors acknowledge the assistance of Sonia Watson, PhD, in editing the manuscript.

Abstract

Recognition of key concepts of structural and functional anatomy of the cerebellum can facilitate image interpretation and clinical correlation. Recently, the human brain mapping literature has increased our understanding of cerebellar anatomy, function, connectivity with the cerebrum, and significance of lesions involving specific areas.

Both the common names and numerically based Schmahmann classifications of cerebellar lobules are illustrated. Anatomic patterns, or signs, of key fissures and white matter branching are introduced to facilitate easy recognition of the major anatomic features. Color-coded overlays of cross-sectional imaging are provided for reference of more complex detail. Examples of exquisite detail of structural and functional cerebellar anatomy at 7 Tesla MRI are also depicted.

The functions of the cerebellum are manifold with the majority of areas involved with non-motor association function. Key concepts of lesion-symptom mapping which correlates lesion location to clinical manifestation are introduced, emphasizing that lesions in most areas of the cerebellum are associated with predominantly non-motor deficits. Clinical correlation is reinforced with examples of intrinsic pathologic derangement of cerebellar anatomy and altered functional connectivity due to pathology of the cerebral hemisphere. The purpose of this pictorial review is to illustrate basic concepts of these topics in a cross-sectional imaging-based format that can be easily understood and applied by radiologists.

BJR UNCORRECTED PROOFS

1
2
3
4 **Current Concepts of Cross-Sectional and Functional Anatomy of the Cerebellum: A Pictorial**
5
6 **Review and Atlas**
7
8
9
10
11

12 Running head: Cerebellum: structural, functional and imaging review
13
14
15
16

17 **Abstract**
18
19
20
21
22
23
24
25
26
27

28 Recognition of key concepts of structural and functional anatomy of the cerebellum can facilitate image
29 interpretation and clinical correlation. Recently, the human brain mapping literature has increased our
30 understanding of cerebellar anatomy, function, connectivity with the cerebrum, and significance of
31 lesions involving specific areas.
32
33

34 Both the common names and numerically based Schmahmann classifications of cerebellar lobules are
35 illustrated. Anatomic patterns, or signs, of key fissures and white matter branching are introduced to
36 facilitate easy recognition of the major anatomic features. Color-coded overlays of cross sectional
37 imaging are provided for reference of more complex detail. Examples of exquisite detail of structural
38 and functional cerebellar anatomy at 7 Tesla MRI are also depicted.
39
40

41
42
43
44
45 The functions of the cerebellum are manifold with the majority of areas involved with non-motor
46 association function. Key concepts of lesion-symptom mapping which correlates lesion location to
47 clinical manifestation are introduced, emphasizing that lesions in most areas of the cerebellum are
48 associated with predominantly non-motor deficits. Clinical correlation is reinforced with examples of
49 intrinsic pathologic derangement of cerebellar anatomy and altered functional connectivity due to
50 pathology of the cerebral hemisphere. The purpose of this pictorial review is to illustrate basic concepts
51
52
53
54
55
56
57
58
59
60
61
62
63
64
65

1
2
3
4 of these topics in a cross-sectional imaging-based format that can be easily understood and applied by
5
6 radiologists.
7
8
9
10
11
12
13
14
15
16
17
18
19
20
21
22
23
24
25
26
27
28
29
30
31
32
33
34
35
36
37
38
39
40
41
42
43
44
45
46
47
48
49
50
51
52
53
54
55
56
57
58
59
60
61
62
63
64
65

BJR UNCORRECTED PROOFS

1
2
3
4 **Introduction**
5
6

7 The structural and functional anatomy of the cerebellum is complex, but demonstrates reproducible
8 spatial organization. Detail of cerebellar pathologic derangement is often under-emphasized in
9 radiology education and reports, but recognition of key concepts and patterns can facilitate image
10 interpretation and clinical correlation. In recent decades, advances in the human brain mapping
11 literature has increased our understanding of anatomy, function, and the clinical significance of lesions
12 involving specific areas of the cerebellum. The purpose of this pictorial review is to illustrate basic
13 concepts of these imaging topics to facilitate application to clinical practice and to the appraisal of
14 human brain mapping research. To do this, key patterns, or signs, of white matter branching and fissure
15 prominence, configuration, and orientation are presented to depict the major anatomic features. Color-
16 coded overlays are provided for reference of further anatomic detail. A brief introduction to relevant
17 embryology and correlation to general vascular territories are provided. Functional organization is
18 presented with blood oxygen level dependent (BOLD) fMRI signal and introduction of lesion-symptom
19 mapping.
20
21
22
23
24
25
26
27
28
29
30
31
32
33
34
35
36
37
38
39
40
41
42
43
44
45
46
47
48
49
50
51
52
53
54
55
56
57
58
59
60
61
62
63
64
65

Overview of Cross-Sectional Anatomy

The cerebellum broadly consists of cortex, central white matter, and deep nuclei. The cortex lacks areas of highly distinct cytoarchitecture analogous to the Brodmann areas of the brain. However, differences in biochemistry and function occur within sagittally-oriented segments that have been divided into zones/stripes and modules with a medial to lateral gradient of connectivity to the inferior olives and deep nuclei.¹ The trilaminar cortical layers can be remembered with the mnemonic **MPG** (superficial to deep: **m**olecular, **P**urkinje, and **g**ranular); the molecular and granular layers have been visualized *in vivo* with specialized techniques at 7T, but are not routinely visualized in current clinical practice.² The

1
2
3
4 Purkinje layer is too small to visualize *in vivo* with current techniques, but serves as the cortical output
5
6 to the deep nuclei.
7
8
9

10
11 The central white matter (corpus medullare) has distinct branching patterns (arbor vitae); of these
12 several particularly prominent white matter stems can be used to identify key anatomic areas. The deep
13 nuclei give rise to the major efferent white matter fibers. While the dentate nucleus is commonly
14 visualized at 1.5T or 3T MRI, the interposed and fastigial nuclei are more challenging to visualize even at
15 higher field strength.^{3,4}
16
17
18
19
20
21

22
23
24
25 Side-to-side, the cerebellum is divided into two hemispheres with a midline vermis. Both the
26 hemispheres and the vermis are typically divided into 3 lobes. In turn, fissures subdivide the lobes into
27 numerous lobules (Figs. 1-5). Importantly, the designation of ‘anterior’ and ‘posterior’ location for both
28 the lobes and axis of development (below) reflect ‘cranial’ and ‘caudal’ location respectively rather than
29 designations by conventional clinical MRI terminology. While the radiologist may be familiar with the
30 common names of the lobes and lobules, numerous nomenclature schemes and definitions exist which
31 can create some confusion. To address this variability, Schmahmann et al. proposed a numerical
32 nomenclature which is commonly used in the human brain mapping literature and emerging in the
33 imaging literature.^{5,6} Assessment of this level of detail can be important since function and
34 predisposition to certain pathology varies amongst the lobules. Recognition of lobule anatomy also
35 facilitates assessment of congenital anomalies. The Schmahmann classification simplifies lobule
36 nomenclature as the lobules are arranged in numerical order (I-X) radially in the sagittal plane. In many
37 locations, the lobule can be identified quickly on cross sectional imaging by the relationship to patterns,
38 or signs, of key fissures or white matter stems presented in the figures of this essay. Several methods of
39
40
41
42
43
44
45
46
47
48
49
50
51
52
53
54
55
56
57
58
59
60
61
62
63
64
65

1
2
3
4 automated parcellation of the cerebellar lobules which could aid visual identification and assessment
5
6 have been described, but these are not yet widely evaluated or implemented in clinical practice.⁷
7
8
9
10

11 Embryology 12

13 The development of the cerebellum is highly complex and the details are beyond the scope of this
14 review. Barkovich et al. have provided an in-depth analysis with a comprehensive classification system
15 of congenital anomalies.⁸ In brief, both the cerebellum and brainstem (pons and medulla) are derived
16 from the rhombencephalon. The fissures appear in sequence, with the primary and posterolateral
17 fissures (separating the lobes) developing first while those separating lobules VI, VIIA, and VIIIB (which
18 are the only lobules to share a common white matter stem in the vermis) are the last to form.⁶
19
20 Understanding this sequence can facilitate interpretation of expected findings on prenatal imaging and
21 avert a misdiagnosis of hypoplasia prior to final differentiation of the lobules.⁶ There is both
22 anteroposterior (craniocaudal) and dorsoventral hindbrain patterning; abnormalities of these processes
23 can lead to deranged anatomy along the respective axes.⁸ Importantly, lobular development does not
24 occur in the numeric sequence outlined in the Schmahmann classification. Further, the vermis does not
25 arise from fusion of the cerebellar hemispheres, but is derived from dedicated primordium, with the
26 anterior and posterior segments arising separately.⁶ These concepts can account for numerous
27 categories of deranged anatomy including the existence of segmental vermian abnormalities and the
28 isolated presence of the posterior vermis in some cases of rhomboencephalosynapsis.⁶ Examples of
29 these concepts are included in Fig. 6.
30
31
32
33
34
35
36
37
38
39
40
41
42
43
44
45
46
47
48
49
50
51
52
53
54

Diffusion Tensor Imaging (DTI) and Tractography of White Matter

55 DTI can depict areas of afferent and efferent white matter tracts of the cerebellum as well as some of
56 the major white matter stems within the cerebellum. However, tractography techniques are needed for
57
58
59
60
61
62
63
64
65

1
2
3
4 detailed delineation of the afferent and efferent tracts. Karavasilis et al. report that both crossed and
5 uncrossed components of the afferent tracts [fronto-ponto-cerebellar (FPC), parieto-ponto-cerebellar
6 (PPC), occipito-ponto-cerebellar (OPC) tracts] to the cerebral hemispheres can be identified with
7 tractography.⁹ In distinction, the *uncrossed* fibers of the dentato-rubro-thalamo-cortical tract (DRTC) are
8 most consistently depicted with current DTI and tractography techniques, although crossed fibers are
9 more numerous (Fig. 7).⁹ This is important because the cerebellum and DRTC have a role in many tremor
10 conditions and mapping the DRTC can facilitate functional neurosurgical treatment.

23 Overview of Functional Anatomy

24 The cerebellum contributes to diverse distinct CNS functions including motor, language, working
25 memory, executive function, autonomic, and affect. In general, such function demonstrates organization
26 in a medial to lateral distribution and in a radial distribution amongst the lobules. To a first
27 approximation, both motor and association cerebellar function demonstrate mirror-image organization
28 about the crus I/II expansion.¹⁰ There is also evidence of a small tertiary map near lobule IX.¹⁰ As
29 exceptions, some data indicate lack of cerebellar connectivity to the primary visual and primary auditory
30 cortex.¹⁰ During routine clinical fMRI, cerebellar BOLD activity may be identified within the cerebellum at
31 3T or 7T. Additionally, special coils and techniques to specifically assess cerebellum BOLD activity at 7T
32 have been described (Fig. 8).¹¹

33
34
35 Motor function, and corresponding BOLD activity on fMRI examinations, is largely found in the anterior
36 lobe, with additional motor function within the ventral cerebellum (particularly lobules VIII) and deep
37 cerebellar nuclei. This motor activity demonstrates somatotopic organization both within the cerebellar
38 hemispheres and the dorsal dentate nucleus (the ventral dentate nucleus is thought to serve largely
39

1
2
3
4 non-motor function). Key motor function of the cerebellar cortex is medially located within the anterior
5 lobe.
6
7

8
9
10
11 The majority of the cerebellum specializes in non-motor functions with connectivity to multimodal
12 association areas of cerebral cortex (Fig. 9). The bulk of the cerebellum is comprised of the posterior
13 lobe and the lateral and peripheral most regions are formed by crus I/II. The relatively expansive crus
14 I/II lobules demonstrate connectivity to association cerebral cortex. Overall, the size of regional
15 connections between the cerebellum and cerebrum are relatively proportionate.¹⁰ Specific regions of
16 the cerebellum have been found to participate in intrinsic connectivity networks of the brain such as the
17 default mode, salience, and executive networks.^{12, 13}
18
19
20
21
22
23
24
25
26
27
28
29

30 Language function localizes to the posterior lobe contralateral to the language dominant cerebral
31 hemisphere, usually the right posterior lobe of the cerebellum.¹⁴ Similarly, whereas the right cerebral
32 association areas have a prominent role in visuospatial function, this function localizes to the left
33 posterior cerebellar hemisphere. There is also evidence that working memory function maps to the left
34 posterior cerebellar hemisphere.
35
36
37
38
39
40

41
42
43
44 The deep cerebellar nuclei (Fig. 10) also demonstrate medial-lateral and rostral-caudal functional
45 organization. In general amongst the nuclei, motor function is located medially, with truncal motor
46 control closest to midline and lower extremity control present more off midline. Further, somatotopic
47 organization of motor function has been described within the dorsal dentate nucleus with a rostral (foot
48 activation) to caudal (finger activation) gradient at 7T on group analysis, although some overlap
49 occurred.¹⁵
50
51
52
53
54
55
56
57
58
59
60
61
62
63
64
65

1
2
3
4 **Lesion-Symptom Mapping**
5
6

7 Lesion involving specific regions of the cerebellar hemispheres or deep nuclei can result in specific
8 clinical findings (Fig. 11). However, such findings can be more subtle and variable than with lesions of
9 the cerebral hemispheres and clinically detectable deficit may be absent. Studies in the human brain
10 mapping literature have correlated the area of lesion overlap and involvement to clinical deficits in
11 groups of patients.^{16, 17} In general, the resultant clinical manifestations can be predicted by knowledge
12 of cerebellar functional topology.
13
14

15 For example, lower limb ataxia can result from lesions of lobules III-IV and upper limb ataxia from lesions
16 of lobules IV-VI. Dysarthria can result from lesions of lobules V and VI and eyeblink conditioning is
17 altered by lesions of lobule VI and crus I. Lesions of the deep cerebellar nuclei can also be subdivided,
18 with lesions of the fastigial and interposed nuclei predisposing to truncal ataxia and lesions of the
19 interposed and dentate nuclei predisposing to limb ataxia. In general, there seems to be less recovery of
20 function in the chronic state with lesions of the deep nuclei relative to the cortex.^{16, 17}
21
22

23 Isolated acute cerebellar infarcts can provide insight into cerebellar function due to acute onset, lack of
24 opportunity to adapt, and defined anatomic extent of pathology. Anterior lobe infarcts, which
25 approximately correspond to the superior cerebellar artery (SCA) territory, can result in predominantly
26 motor symptoms including dysarthria and upper and/or lower limb ataxia depending on location (Fig
27 11). The SCA also typically supplies the dorsal (motor) portions of the dentate nucleus whereas the
28 posterior inferior cerebellar artery (PICA) supplies the inferior (nonmotor dentate); accordingly evidence
29 indicates the SCA infarcts with dentate involvement are associated with impaired hand gripping tests
30 whereas PICA infarcts with dentate involvement are not.¹⁸ However, the majority of cerebellar infarcts
31 involve the posterior lobe (approximately anterior inferior cerebellar artery (AICA)-PICA territory), which
32
33

1
2
3
4 may be associated with predominantly nonspecific symptoms including nausea, headache, and
5
6 confusion. Although the correlation of loss of function to area of isolated cerebellar infarct somewhat
7
8 variable, in general limb ataxia and dysarthria are most common with SCA infarcts whereas gait ataxia
9 can be seen with SCA or PICA infarcts, in particular with involvement of the vermis.^{17, 19, 20}

10
11
12
13
14
15
16 Lesion-symptom mapping can also be predicated upon longer-standing pathology and the effects of
17 surgical resection. For example, there is evidence that resection of tumors from the posterior lobes can
18 result in impaired cognition, affect, and pain processing and that resection of medulloblastomas of the
19 left posterior cerebellar lobe is associated with decreased working memory.^{21, 22} Schmahmann et al.
20 described the cerebellar cognitive affective disorder (CCAS), which encompasses a variety of executive
21 function and behavioral symptoms due to lesions of the posterior lobes.¹⁶ This can include planning,
22 reasoning, working memory, language, personality, affect, and altered behavior.

31
32
33
34
35 **Pathologic Derangement**

36
37 With symptom-lesion mapping, study of normal function and structure can facilitate an understanding
38 of clinical manifestations of pathology. Both intrinsic derangement within the cerebellum itself and
39 altered functional connectivity due to pathology of the cerebral hemisphere are possible. Altered
40 structure and function can be on either an acquired or a congenital basis (Figs. 12-13).

41
42
43
44
45
46
47
48
49
50
51
52 **Key Take Home Points:**

- 53
54 1. Advances in the human brain mapping literature in recent decades have substantially improved
55
56 the understanding of cross-sectional and functional anatomy of the cerebellum.

- 1
2
3
4 2. Numerical lobule designation per the Schmahmann classification is arranged radially in the
5 sagittal plane. Most lobules of the vermis are identified by an independent white matter stem,
6 whereas lobules VI, VIIA, and VIIB have a common dorsally-directed stem and are the last to
7 differentiate.
8
9 3. The main anatomic features of the cerebellum on MRI can be recognized by relationship to
10 several typical white matter stem and fissure configurations, orientations, and/or prominence.
11 Key signs include the '**intraculminate X sign**' just anterior to the deep primary fissure and the
12 '**crus I bowtie sign**' amongst many others described herein.
13
14 4. Lesion-symptom mapping reports indicate that lesions of the anterior lobe can result
15 predominantly in motor deficits and specific forms of ataxia corresponding to homunculus
16 involvement whereas lesions of the larger posterior lobe can result in nonmotor symptoms such
17 as CCAS and impaired working memory. Nonetheless lesions of the cerebellum often result in a
18 variety of non-specific symptoms. Lesions of the deep nuclei are important to recognize since
19 there is generally less recovery of function over time compared to other regions of the
20 cerebellum.
21
22 5. The cerebellum plays a role in tremor syndromes and DRTC tractography, including that of
23 uncrossing fibers, can facilitate functional neurosurgical treatment.
24
25 6. Normal and pathologic anatomy and function of the cerebellum is intertwined with the
26 brainstem and cerebrum via circuits. Cerebellar pathology can arise from insults primary to
27 these other locations such as malformations of cerebral cortical development.

1
2
3
4
5
6 **References**
7

- 8
9 1. Apps R, Hawkes R, Aoki S, Bengtsson F, Brown AM, Chen G, et al. Cerebellar Modules
10 and Their Role as Operational Cerebellar Processing Units: A Consensus paper [corrected].
11 Cerebellum. 2018;17(5):654-82.
12
13 2. Marques JP, van der Zwaag W, Granziera C, Krueger G, Gruetter R. Cerebellar cortical
14 layers: in vivo visualization with structural high-field-strength MR imaging. Radiology.
15 2010;254(3):942-8.
16
17 3. Diedrichsen J, Maderwald S, Kuper M, Thurling M, Rabe K, Gizewski ER, et al. Imaging
18 the deep cerebellar nuclei: a probabilistic atlas and normalization procedure. Neuroimage.
19 2011;54(3):1786-94.
20
21 4. Maderwald S, Thurling M, Kuper M, Theysohn N, Muller O, Beck A, et al. Direct
22 visualization of cerebellar nuclei in patients with focal cerebellar lesions and its application for
23 lesion-symptom mapping. Neuroimage. 2012;63(3):1421-31.
24
25 5. Schmahmann JD, Doyon J, Petrides M, Evans A, Toga A. MRI Atlas of the Human
26 Cerebellum: Academic Press, 2000.
27
28 6. Robinson AJ. Inferior vermian hypoplasia--preconception, misconception. Ultrasound
29 Obstet Gynecol. 2014;43(2):123-36.
30
31 7. Yang Z, Ye C, Bogovic JA, Carass A, Jedynak BM, Ying SH, et al. Automated cerebellar
32 lobule segmentation with application to cerebellar structural analysis in cerebellar disease.
33 Neuroimage. 2016;127:435-44.
34
35
36
37
38
39
40
41
42
43
44
45
46
47
48
49
50
51
52
53
54
55
56
57
58
59
60
61
62
63
64
65

- 1
2
3
4 8. Barkovich AJ, Millen KJ, Dobyns WB. A developmental and genetic classification for
5 midbrain-hindbrain malformations. *Brain*. 2009;132(Pt 12):3199-230.
6
7 9. Karavasilis E, Christidi F, Velonakis G, Giavri Z, Kelekis NL, Efstathopoulos EP, et al.
8 Ipsilateral and contralateral cerebro-cerebellar white matter connections: A diffusion tensor
9 imaging study in healthy adults. *J Neuroradiol*. 2019;46(1):52-60.
10
11 10. Buckner RL, Krienen FM, Castellanos A, Diaz JC, Yeo BT. The organization of the human
12 cerebellum estimated by intrinsic functional connectivity. *J Neurophysiol*. 2011;106(5):2322-45.
13
14 11. Batson MA, Petridou N, Klomp DW, Frens MA, Neggers SF. Single session imaging of
15 cerebellum at 7 Tesla: obtaining structure and function of multiple motor subsystems in
16 individual subjects. *PLoS One*. 2015;10(8):e0134933.
17
18 12. Bernard JA, Seidler RD, Hassevoort KM, Benson BL, Welsh RC, Wiggins JL, et al. Resting
19 state cortico-cerebellar functional connectivity networks: a comparison of anatomical and self-
20 organizing map approaches. *Front Neuroanat*. 2012;6:31.
21
22 13. Habas C, Kamdar N, Nguyen D, Prater K, Beckmann CF, Menon V, et al. Distinct
23 cerebellar contributions to intrinsic connectivity networks. *J Neurosci*. 2009;29(26):8586-94.
24
25 14. Jansen A, Floel A, Van Randenborgh J, Konrad C, Rotte M, Forster AF, et al. Crossed
26 cerebro-cerebellar language dominance. *Hum Brain Mapp*. 2005;24(3):165-72.
27
28 15. Kuper M, Thurling M, Stefanescu R, Maderwald S, Roths J, Elles HG, et al. Evidence for a
29 motor somatotopy in the cerebellar dentate nucleus--an fMRI study in humans. *Hum Brain*
30
31 Mapp. 2012;33(11):2741-9.

- 1
2
3
4 16. Stoodley CJ, MacMore JP, Makris N, Sherman JC, Schmahmann JD. Location of lesion
5 determines motor vs. cognitive consequences in patients with cerebellar stroke. Neuroimage
6
7 Clin. 2016;12:765-75.
- 8
9 17. Timmann D, Brandauer B, Hermsdorfer J, Ilg W, Konczak J, Gerwig M, et al. Lesion-
10 symptom mapping of the human cerebellum. Cerebellum. 2008;7(4):602-6.
- 11
12 18. Kim S, Lee H, Lee Y, Lee J, Yang J, Lee M, et al. Blood Supply by the Superior Cerebellar
13 Artery and Posterior Inferior Cerebellar Artery to the Motor and Nonmotor Domains of the
14 Human Dentate Nucleus. World Neurosurg. 2019;122:e606-e11.
- 15
16 19. De Cocker LJ, Geerlings MI, Hartkamp NS, Grool AM, Mali WP, Van der Graaf Y, et al.
17 Cerebellar infarct patterns: The SMART-Medea study. Neuroimage Clin. 2015;8:314-21.
- 18
19 20. Deluca C, Moretto G, Di Matteo A, Cappellari M, Basile A, Bonifati DM, et al. Ataxia in
21 posterior circulation stroke: clinical-MRI correlations. J Neurol Sci. 2011;300(1-2):39-46.
- 22
23 21. Hoang DH, Pagnier A, Cousin E, Guichardet K, Schiff I, Iché C, et al. Anatomo-functional
24 study of the cerebellum in working memory in children treated for medulloblastoma. J
25 Neuroradiol. 2019;46(3):207-13.
- 26
27 22. Silva KE, Rosner J, Ullrich NJ, Chordas C, Manley PE, Moulton EA. Pain affect disrupted in
28 children with posterior cerebellar tumor resection. Ann Clin Transl Neurol. 2019;6(2):344-54.

1
2
3
4 **Figure Legends**
5
6
7
8
9

10 **Figure 1.** Illustration of the lobes and lobules of the cerebellum with both common names and
11 enumeration per the Schmahmann classification. The color patterns of the lobules and fissures match
12 those in subsequent figures. Note that the precise definitions and nomenclature of individual lobules
13 and even the lobes vary in the literature.
14
15
16
17
18
19
20

21 **Figure 2.** Three-dimensional surface shaded images of the cerebellum. The superior view demonstrates
22 the general relationship of lobules III to Crus I and the position of the primary fissure. Note the relatively
23 small size of the anterior lobe. The vermis of the anterior lobe is incorporated into the hemispheres and
24 not truly separated. The superior posterior fissure is also prominent. The posterior view demonstrates
25 prominent superior posterior and horizontal fissures that converge near the posterior midline (B). These
26 fissures bracket the bilateral Crus I, resulting in a ‘bowtie’ appearance (**Crus I Bowtie Sign**). The bulk of
27 the periphery of the cerebral hemispheres is comprised of Crus I and Crus II, and to a lesser extent
28 lobule VIIB. The remaining lobules are smaller and more medial in location. An inferior view of the
29 cerebellum demonstrates the flocculus (lobule X) and the tonsil of lobule IX as well as lobules VIII and
30 VIIIB (C). An anterior view demonstrates the relative position of all the lobules (I-X) of the cerebellar
31 hemispheres and the anterior vermis including the nodulus (lobule X) (D).
32
33
34
35
36
37
38
39
40
41
42
43
44
45
46
47
48

49 **Figure 3.** Key sagittal magnetization-prepared rapid acquisition with gradient echo (MPRAGE) views of
50 the cerebellum, medial to lateral at 3T (A-D) and 7T (E-F). Near-midline sagittal view demonstrates the
51 vermis in native (A) and color-coded, enumerated (B) formats. The **deep midline primary (light blue)**
52 and **prepyramidal/prebiventral (dark blue)** fissures are prominent features of a normal vermis. The
53 primary fissure separates the anterior lobe (lobules I-V) from the posterior lobe (lobules VI-IX, with
54
55
56
57
58
59
60
61
62
63
64
65

1
2
3
4 lobule X constituting the flocculonodular lobe); note that the ‘anterior’ lobe is actually positioned
5
6 superior to the posterior lobe by conventional directions used in clinical interpretation. A common
7
8 **dorsally directed white matter stem (red line) gives rise to lobules VI and VIIA/VIIB**, whereas the
9 remaining lobules of the vermis typically have unique white matter stems. In the mid aspect of the
10 cerebellar hemisphere, the primary fissure is shallow and anteriorly positioned, consistent with
11 relatively small and medial configuration of the anterior lobe (C). The white matter stems of the crus I
12 (yellow) and crus II (light blue) are clearly distinguishable. The superior posterior and horizontal fissures
13 bracket crus I. The far lateral aspect of the cerebellar hemisphere is composed of the crus I/crus II
14 expansions along with lobule VIIB (D). The superior posterior and horizontal fissures remain clearly
15 visible and converge anteriorly. Sagittal images in another patient at 7T demonstrates a very similar
16 appearance of the lobules and major fissures of the vermis (E) and the lateral cerebellar hemisphere (F)
17 with only minor differences compared to the first patient, illustrating that these features are reasonably
18 reproducible. Although the fine detail of the lobules and fissures are better depicted at 7T, note that the
19 main features are also readily identifiable at 3T.
20
21
22
23
24
25
26
27
28
29
30
31
32
33
34
35
36
37
38
39
40

41 **Figure 4.** Key axial MPRAGE (A-C) and corresponding T2 weighed (D-F) views of the cerebellum at 7T,
42 superior to inferior. In the superior cerebellum, the intraculminate fissures terminate medially in an ‘X-
43 shaped’ region (**‘Intraculminate X’ sign**) of white matter (A). In distinction, the primary fissure is
44 relatively deep and continues to extend across midline at this level just posterior the ‘X.’ In the mid-
45 cerebellum, the white matter stems of crus I (yellow) and crus II (blue) converge medially to form a
46 sideways ‘horseshoe’ configuration (**‘Crus Horseshoe’ sign**) surrounding the horizontal fissure (B).
47 Within the vermis, a ‘diamond’ configuration of white matter (**‘Diamond’ Sign**) demarcates the locations
48 of the white matter stems to lobules VIII (posterior diamond) and IX (anterior diamond). Lobule X (the
49 nodulus) makes an impression on the fourth ventricle and is flanked by superior portions of the
50
51
52
53
54
55
56
57
58
59
60
61
62
63
64
65

1
2
3
4 cerebellar tonsils (lobule IX). The **relatively deep/prominent prepyramidal/prebiventral fissure** has a
5 characteristic appearance with **upturned anteriorly directed edges**, just posterior to the 'diamond' of
6 white mater. The biventral lobules form the ventral surface of the cerebellar hemispheres (C). The
7 tonsils (lobule IX) extend inferomedially. Inferiorly, the **horizontal fissure** has a slight **medial convex**
8 orientation. These same features can also be recognized on high-resolution T2 weighted images,
9 although the white matter stems demonstrate hypointense signal rather than the hyperintense signal
10 seen on T1 weighted images. Note that the hypointense white matter stem to lobule IX of the cerebellar
11 hemisphere (white arrow) is slightly outwardly convex whereas the white matter stems to lobules VIIIB
12 (orange arrow), VIIIA (yellow arrow), and VIIB (blue arrow) are inwardly convex (F).

13
14
15
16
17
18
19
20
21
22
23
24
25
26
27
28 **Figure 5.** Key coronal views of the cerebellum, posterior to anterior at 3T (A-D) and 7T (E). Posteriorly,
29 the cerebellum is comprised predominantly of the crus I and crus II expansions (A). The **white matter**
30
31 **stems to crus I and crus II** are well-defined and **converge posteromedially** along with the superior
32 posterior and horizontal fissures. In the mid-posterior plane (B), the primary fissure is prominent and is
33 continuous across midline (there is not a truly separate vermis superiorly in the mature cerebellum). The
34 intraculminate fissure is also seen extending across midline superiorly. The mid cerebellum
35 demonstrates the majority of the lobules of the cerebellar hemispheres (C). Along the basal cerebellum,
36 the **prepyramidal/prebiventral fissure** typically has a slight **superomedial slant** while the **secondary**
37 **fissure** has a **superolateral slant**. A posterior image demonstrates lateral shallow positions of the
38 intraculminate and primary fissure (D). The nodulus (lobule X) is also visualized. A coronal T2 weighted
39 image at 7T in another patient at a posterior level (similar level to B) demonstrates that the major white
40 matter stem branching pattern is reproducible, with prominent T2 hypointense white matter stems to
41 crus I and crus II that converge medially and a moderately prominent stem to lobule VI.
42
43
44
45
46
47
48
49
50
51
52
53
54
55
56
57
58
59
60
61
62
63
64
65

1
2
3
4 **Figure 6.** Congenital anomalies of the cerebellum in three patients. First, a 53-year-old female with
5 extension of cerebellar hemisphere folia continuously across midline with absent vermis indicating
6 classic rhombencephalosynapsis, an abnormality of dorsoventral patterning (A-C).⁸ The superior
7 cerebellar peduncles are fused posteriorly (white arrows, A) and the deep cerebellar nuclei appear fused
8 (white arrows, B). Inferiorly, the vermis is completely absent (C), although in cases of incomplete
9 rhomboencephalosynapsis, the inferior vermis is present. This condition is associated with highly
10 variable cognitive and motor deficits. This patient was a high-functioning professional with mild ataxia
11 on exam. Another case demonstrates vermian hypoplasia in a 5-year-old (D). The vermis is small with
12 superiorly positioned inferior border (white arrows); a dorsally-directed white matter stem consistent
13 with a stem to lobules VI, VIIa, and VIIb flanked by the prominent primary and
14 prepyramidal/prebiventral fissures are present while the lobules while the number of white matter
15 stems to the remaining areas of the anterior and posterior lobe are more difficult to identify. On overall
16 semblance of typical lobulation remains present, compatible with hypoplasia whereas lack of normal
17 lobulation would indicate dysgenesis. A third case demonstrates hypoplasia of both the cerebellum and
18 pons in a 1-year-old (E-F). The vermis is hypoplastic and the pons is markedly hypoplastic (E). Laterally
19 on the right, the cerebellar hemisphere is also small, although the fissures are not widened (F);
20 decreased size due to widening of otherwise normal fissures would indicate atrophy rather than
21 hypoplasia. Note that the white matter stems to crus I and crus II remain identifiable. Hypoplasia of the
22 pons frequently accompanies that of the cerebellum due to shared developmental origins and/or white
23 matter circuitry.⁸

24
25
26
27
28
29
30
31
32
33
34
35
36
37
38
39
40
41
42
43
44
45
46
47
48
49
50
51
52
53
54
55
56
57
58
59
60
61
62
63
64
65

Figure 7. Tractography at the level of the anterior commissure-posterior commissure line demonstrates
the DRTC (purple) at the level of the inferior Ventral Intermediate Nucleus (VIM), the somatomotor tract
(yellow), and somatosensory/medial lemniscus fibers (red) near the ventral caudal nucleus in the

1
2
3
4 thalamus in a patient with right essential tremor (A). Note the close proximity of these three tracts. The
5 VIM was successfully targeted by MRI guided focused ultrasound for treatment of right essential tremor,
6 avoiding the other two tracts. Although most white matter fibers to the DRTC arise from the
7 contralateral cerebellar nuclei, current standard clinical DTI/tractography techniques most often identify
8 fibers arising from the *ipsilateral* dentate nucleus via the ipsilateral superior cerebellar peduncle.
9
10 Directionally-encoded fractional anisotropy images demonstrate a region of dark purple color (lavender
11 arrow) within the thalamus that corresponds to the DRTC and the somatosensory fibers (B), although
12 these two tracts cannot be confidently differentiated; this is just medial to the posterior limb of the
13 internal capsule, which is blue (blue arrow), while the thalamus anterior and medial to this region is
14 green. At the level of the upper midbrain (C), most fibers of the DRTC extend across midline within the
15 decussation of the superior cerebellar peduncles (red arrow), although some fibers remain ipsilateral. At
16 the level of the superior cerebellar peduncles (D), efferent cerebellar white matter tracts, including the
17 DRTC, are seen in light blue color (white arrow). Just inferior to this (E), the DRTC fibers merge with a
18 green area in this patient (color varies amongst patients) (white arrow) along the medial aspect of the
19 dentate nucleus. At this level, red transverse pontine fibers containing the FPC, PPC, and OPC tracts are
20 also visualized (yellow arrow) as well as the middle cerebellar peduncle (green arrow). In the mid to
21 inferior cerebellum, the white matter stems to crus I and crus II are often seen as green tracts (orange
22 arrow denotes stem to crus II) (F).

23
24
25
26
27
28
29
30
31
32
33
34
35
36
37
38
39
40
41
42
43
44
45
46
47
48
Figure 8. BOLD activity in the cerebellum derived from clinical fMRI examinations at 3T and 7T.

50 Somatotopic organization of motor function of the anterior cerebellum lobe can be resolved at 3T (A).
51 Tongue activation (green) is seen posteriorly near the primary fissure (blue arrow), toe tapping
52 (magenta) activation is seen anteriorly, and activation related to finger tasks is seen in the mid-portion
53 of the anterior lobe. This follows the cerebellar homunculus. Motor activity in the anterior cerebellar
54
55
56
57
58
59
60
61
62
63
64
65

hemisphere can be exquisitely demonstrated with bilateral hand clenching at 7T (B). Silent word generation produces activity consistent with bilateral lip motor function in the bilateral anterior lobes at 3T (C). Expressive language tasks also often produce tongue/lip motor activation thought to be related to 'silent word' generation during the task (yellow). Left occipital lobe visual cortex activity also incidentally depicted. Additional language tasks (rhyming task = blue; reading comprehension task = green; semantic decision task = magenta; silent word generation task = yellow) with activity co-localizing to right posterior cerebellar lobe spanning crus I and II (same patient as C) (D). This patient has strong left cerebral hemisphere language dominance on fMRI (not shown).

Figure 9. Color-coded illustration of approximate pattern of *general* regions of connectivity between the cerebral and cerebellar hemispheres, including a 3D-rendered image based on MPRAGE (A), a select coronal (B) and a select axial (C) image from the same patient. Regions of matching color in the cerebrum and cerebellum have been shown to have functional connectivity. Note connectivity of the somatomotor areas to the anterior lobe and lobules VIII and larger areas of connectivity of multimodal association areas to the lateral expansive portions of the cerebellar hemispheres. According to and modified from Buckner et al.¹⁰

Figure 10. Cerebellar nuclei are hypointense on susceptibility weighted imaging (SWI) at 7T. The dentate nucleus is well-delineated while the general locations of the other nuclei can be inferred on visual inspection. The paired fastigial nuclei are near midline, located along the roof of the 4th ventricle (white arrow) (A). The interposed nuclei (globose and emboliform) are not always distinguishable, but located near the dorso-medial border of the dentate nucleus and should be approximated by the labelled structure (white arrow) (B). Ventrally, the normal peripherally-crenulated appearance of the dentate nuclei is well seen (white arrow) (C). An incidental cavernous malformation in the pons is also present.

1
2
3
4
5
6 **Figure 11.** Key approximate areas identified in cerebellar lesion-symptom mapping literature on axial 7T
7 MPRAGE images (A-D). Motor manifestations predominantly involve the anterior lobe and can be
8 roughly predicted by knowledge of somatotopic organization. The upper limb ataxia region primarily
9 involves the anterior lobe, but extends slightly over the primary fissure to the posterior lobe. Cerebellar
10 dysarthria and abnormal eyeblink conditioning reportedly extend across the primary fissure. Eyeblink
11 conditioning has also been mapped to crus I. Truncal ataxia maps to the medial cerebellum throughout
12 the majority of the vermis. Non-motor consequences such as CCAS map to areas of the posterior lobe.
13 The intraculminate (black arrow), primary (white arrow), and horizontal (peach arrow) fissures as well as
14 the white matter stems to crus I (yellow arrow) and crus II (blue arrow) are labelled. Images are
15 modified from Timmann et al.¹⁷

16
17
18
19
20
21
22
23
24
25
26
27
28
29
30
31
32

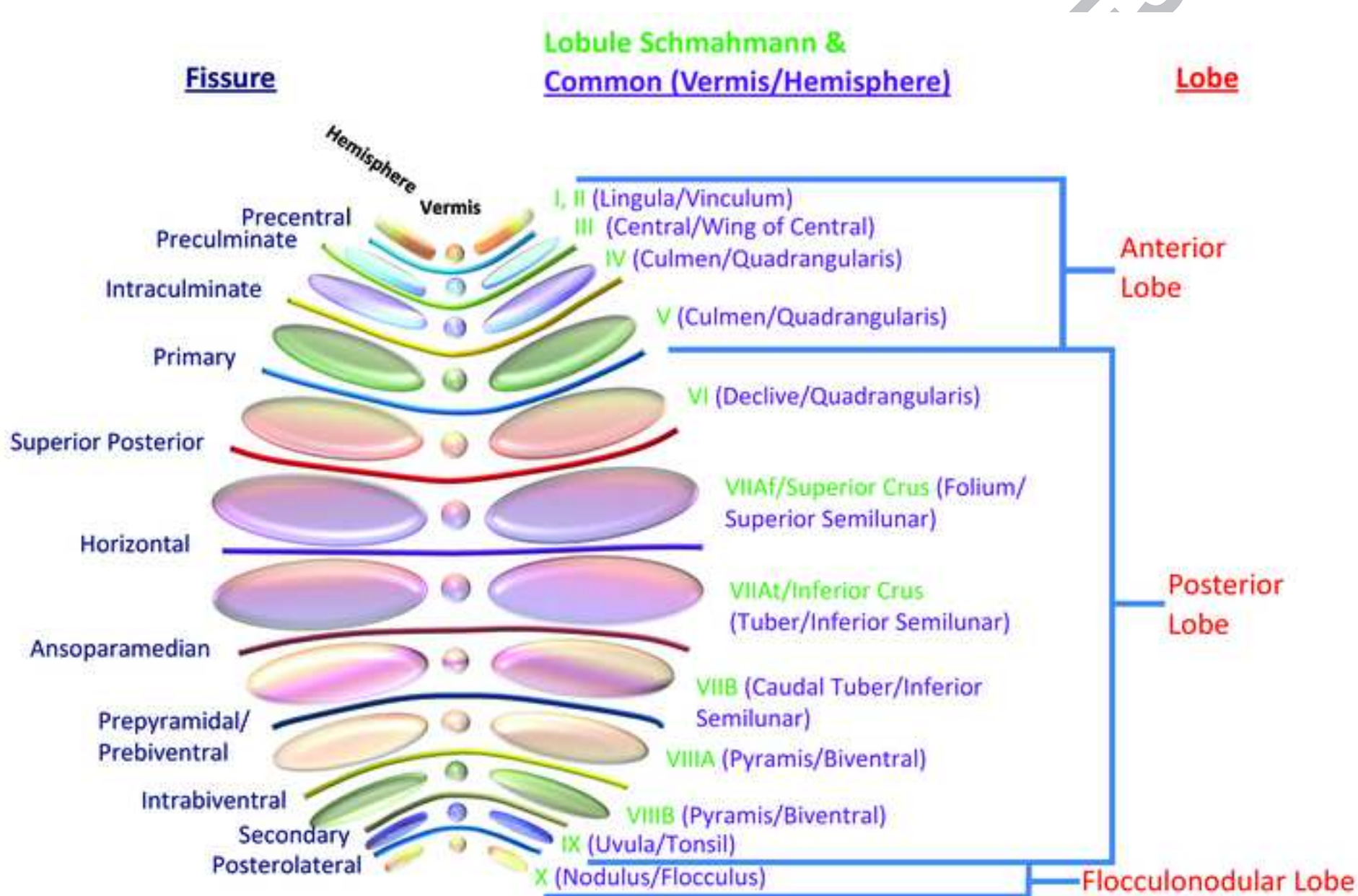
33 **Figure 12.** Example of altered cerebral-cerebellar functional connectivity due to a congenital lesion in
34 the cerebral hemisphere. This patient has schizencephaly in the right primary somatomotor region
35 (arrow) (A,B). BOLD activity on motor tasks indicates that both right and left somatomotor function (red
36 = bilateral finger task with alternating sides, green = tongue task, blue = lip task) is served by the
37 anatomically normal left cerebral hemisphere (A,B). There was no evidence of neurovascular uncoupling
38 in the right cerebral hemisphere (not shown). Corresponding BOLD activity is present in the right
39 cerebellar hemisphere, with bilateral finger tapping depicted (red) (C). There was no appreciable BOLD
40 activity in the expected somatomotor areas of the right cerebral or left cerebellar hemispheres.
41
42
43
44
45
46
47
48
49
50
51
52
53

54 **Figure 13.** Decreased size of a cerebellar nucleus due to involvement with pathology of a brainstem-
55 cerebellum circuit (triangle of Mollaret) with associated decreased accumulation of gadolinium.
56 Asymmetrically T1 hyperintense dentate nucleus in a 32-year-old female with history of right
57
58
59
60
61
62
63
64

1
2
3
4 hypertrophic olivary degeneration and administration of multiple IV gadolinium doses. The right dentate
5 nucleus demonstrates T1 hyperintensity (white arrow) which can be seen after gadolinium
6 administration, and normal size. The left dentate nucleus is atrophic and difficult to visualize, consistent
7 with involvement with hypertrophic olivary degeneration, and demonstrates less intense T1 signal.
8
9
10
11
12
13
14
15
16
17
18
19
20
21
22
23
24
25
26
27
28
29
30
31
32
33
34
35
36
37
38
39
40
41
42
43
44
45
46
47
48
49
50
51
52
53
54
55
56
57
58
59
60
61
62
63
64

65

BJR UNCORRECTED PROOFS



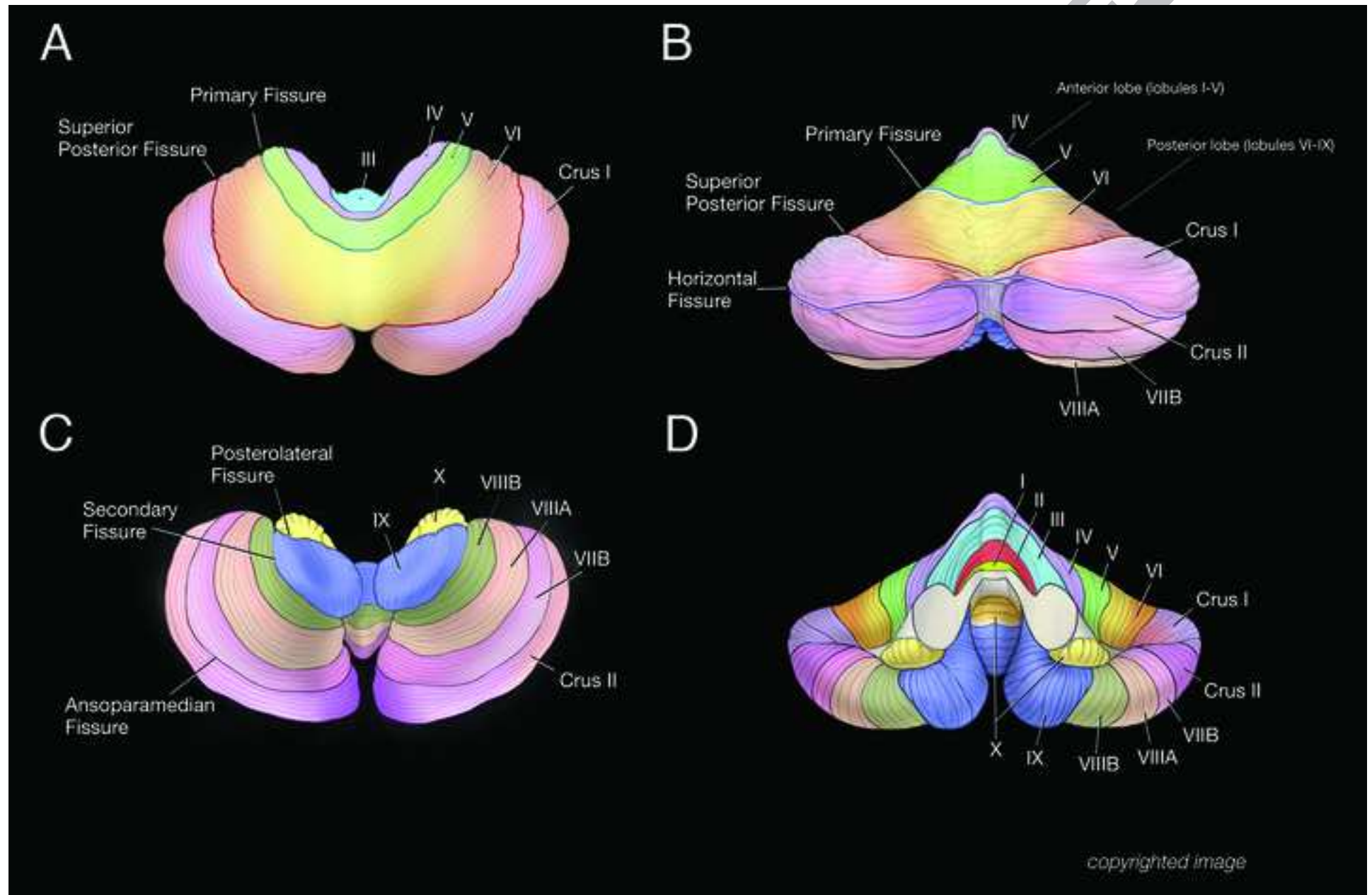


Figure 3

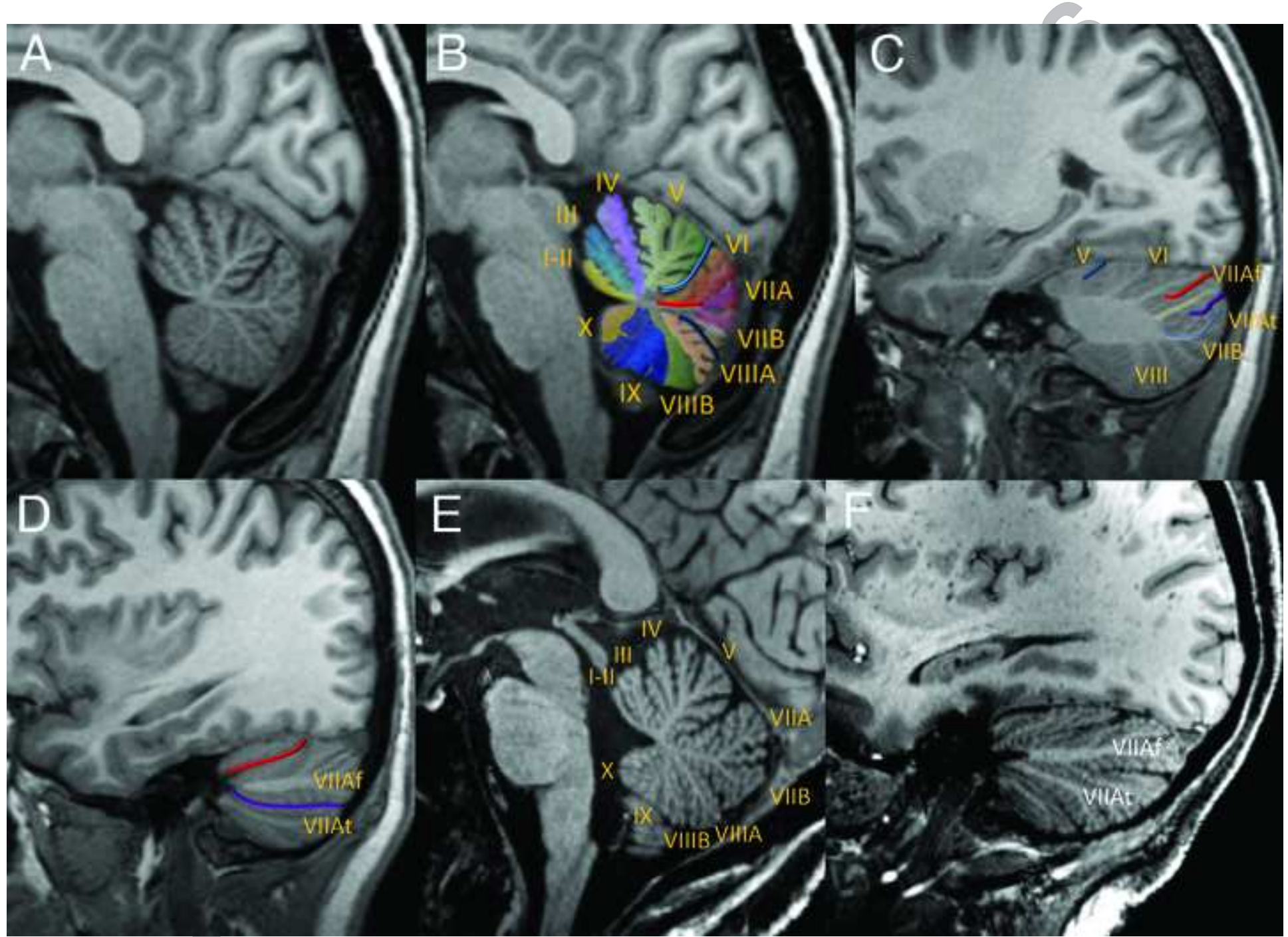
[Click here to access/download;Figure;Fig 3 new flat 300dpi CYMK.tif](#)

Figure 4

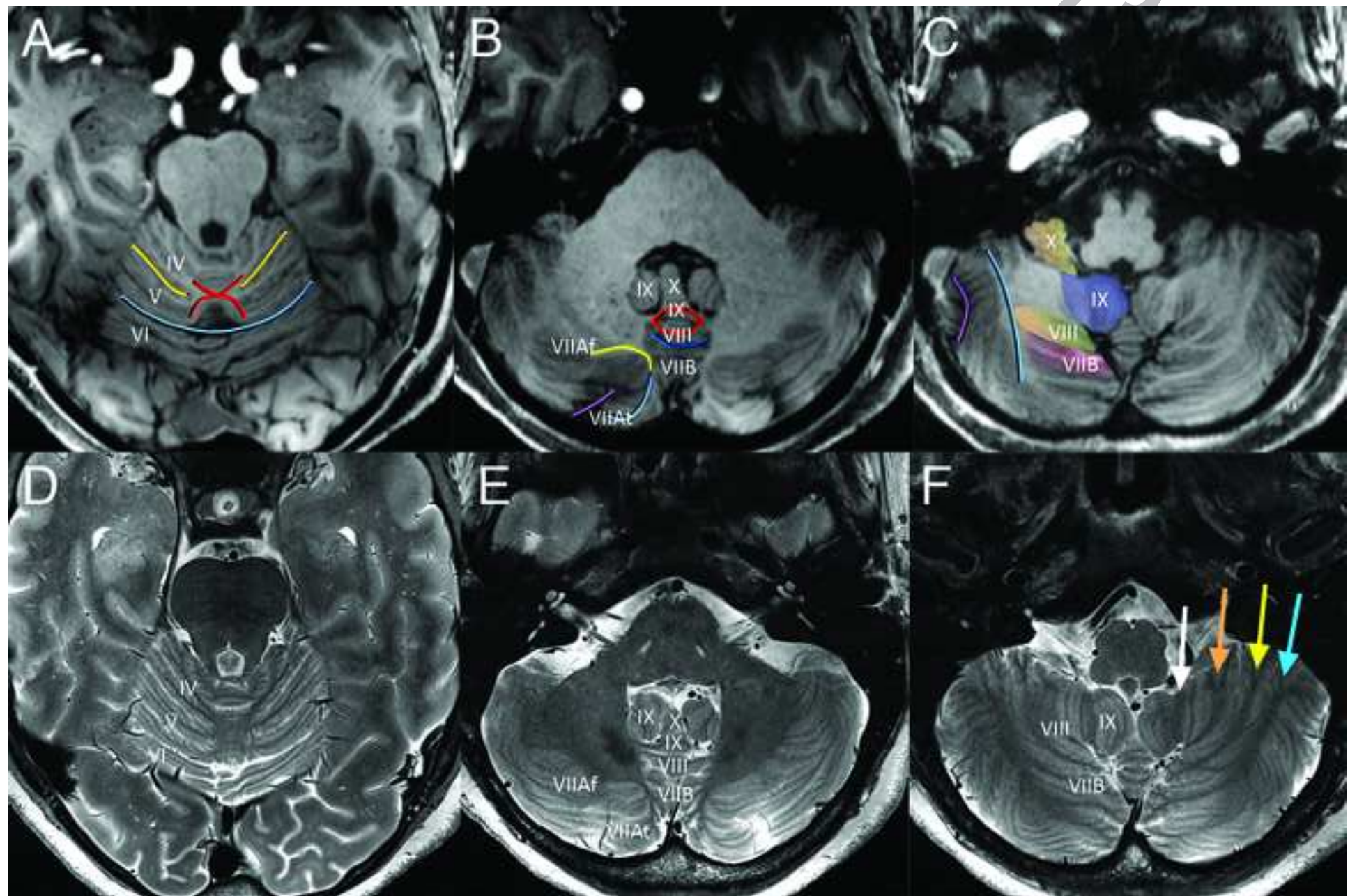
[Click here to access/download;Figure;Fig 4 new c flat 300dpi CYMK.tif](#)

Figure 5

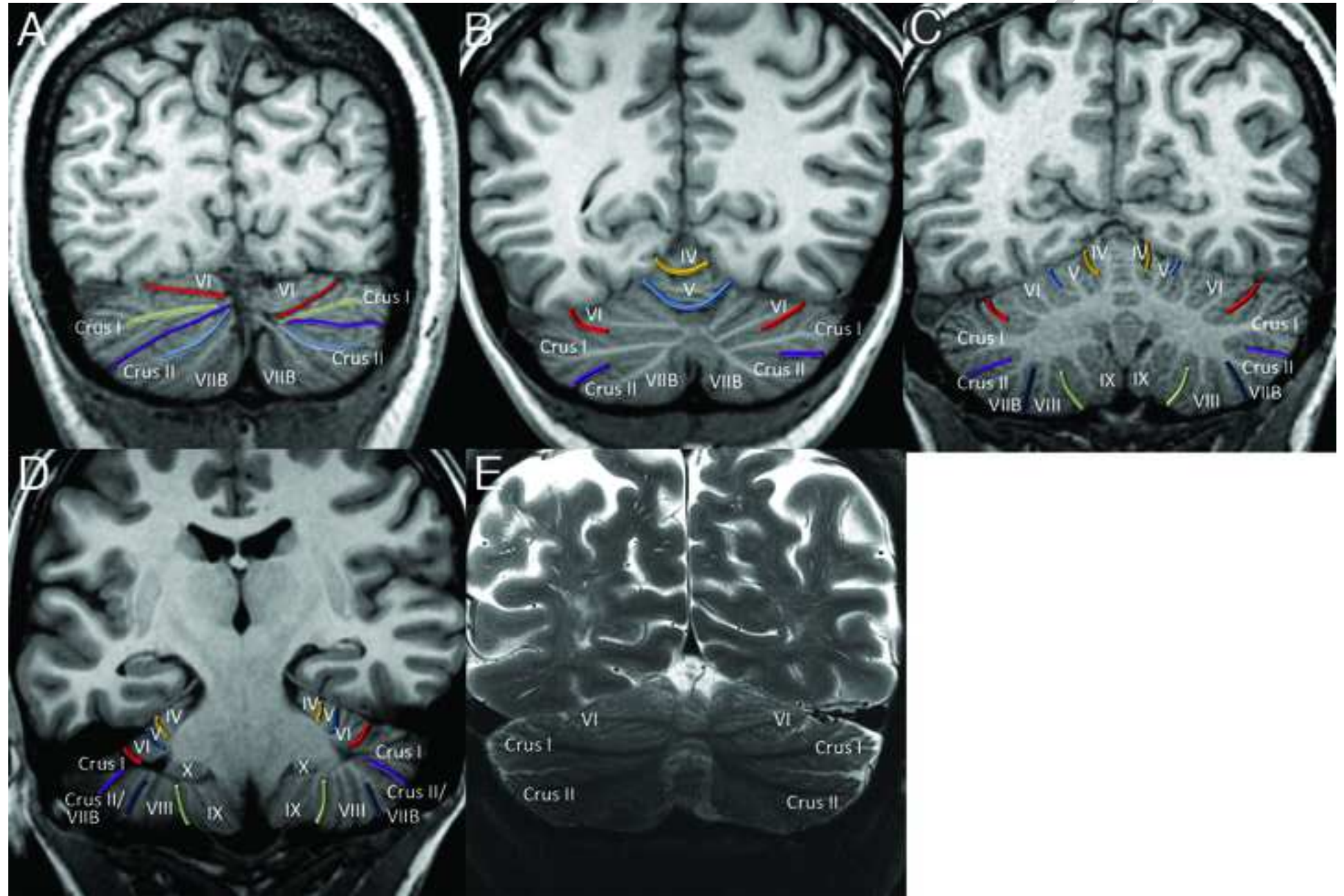
[Click here to access/download;Figure;Fig 5 new flat 300dpi CYMK.tif](#)

Figure 6

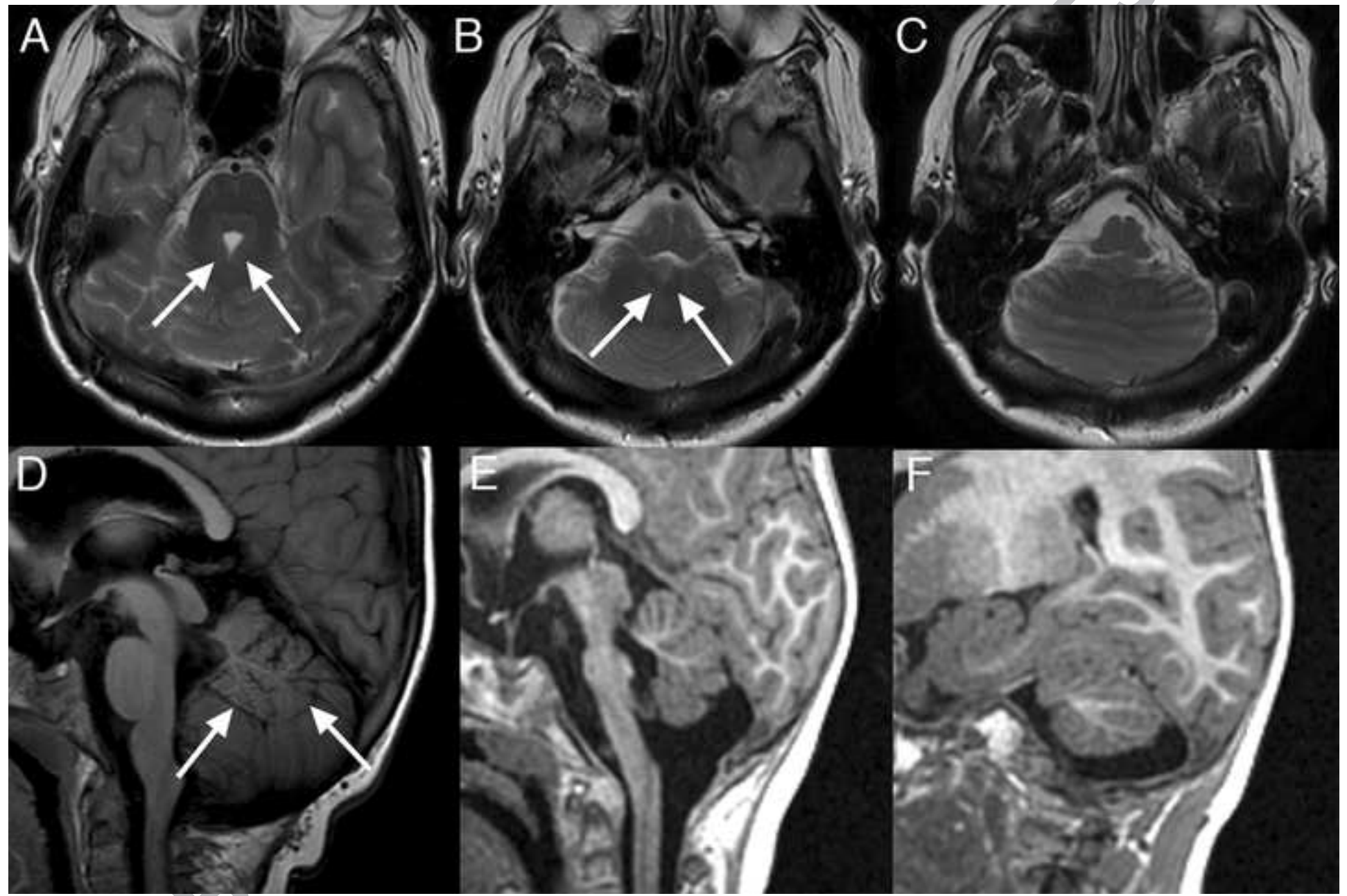
[Click here to access/download;Figure;Fig 6 new flat 300dpi.tif](#)

Figure 7

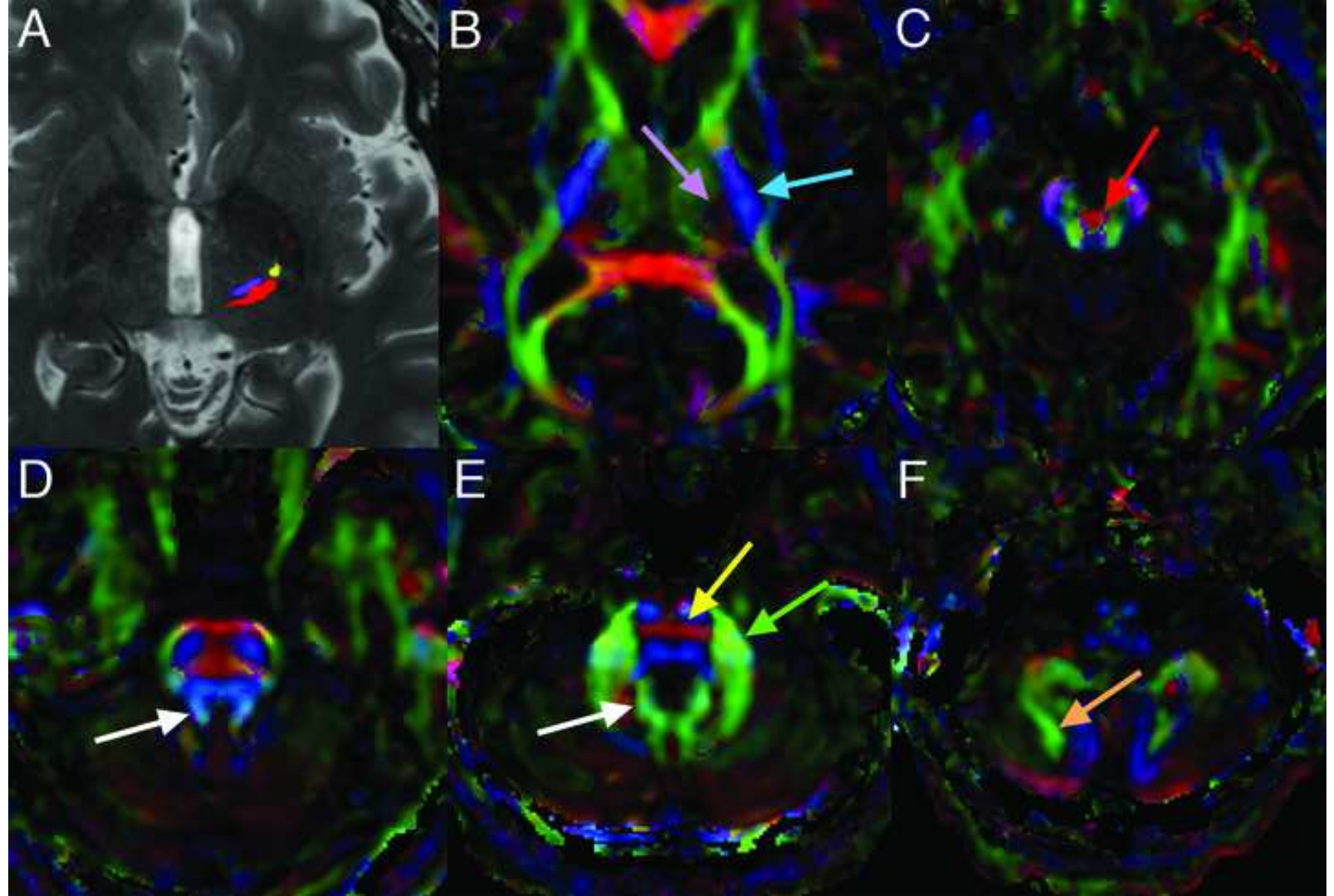
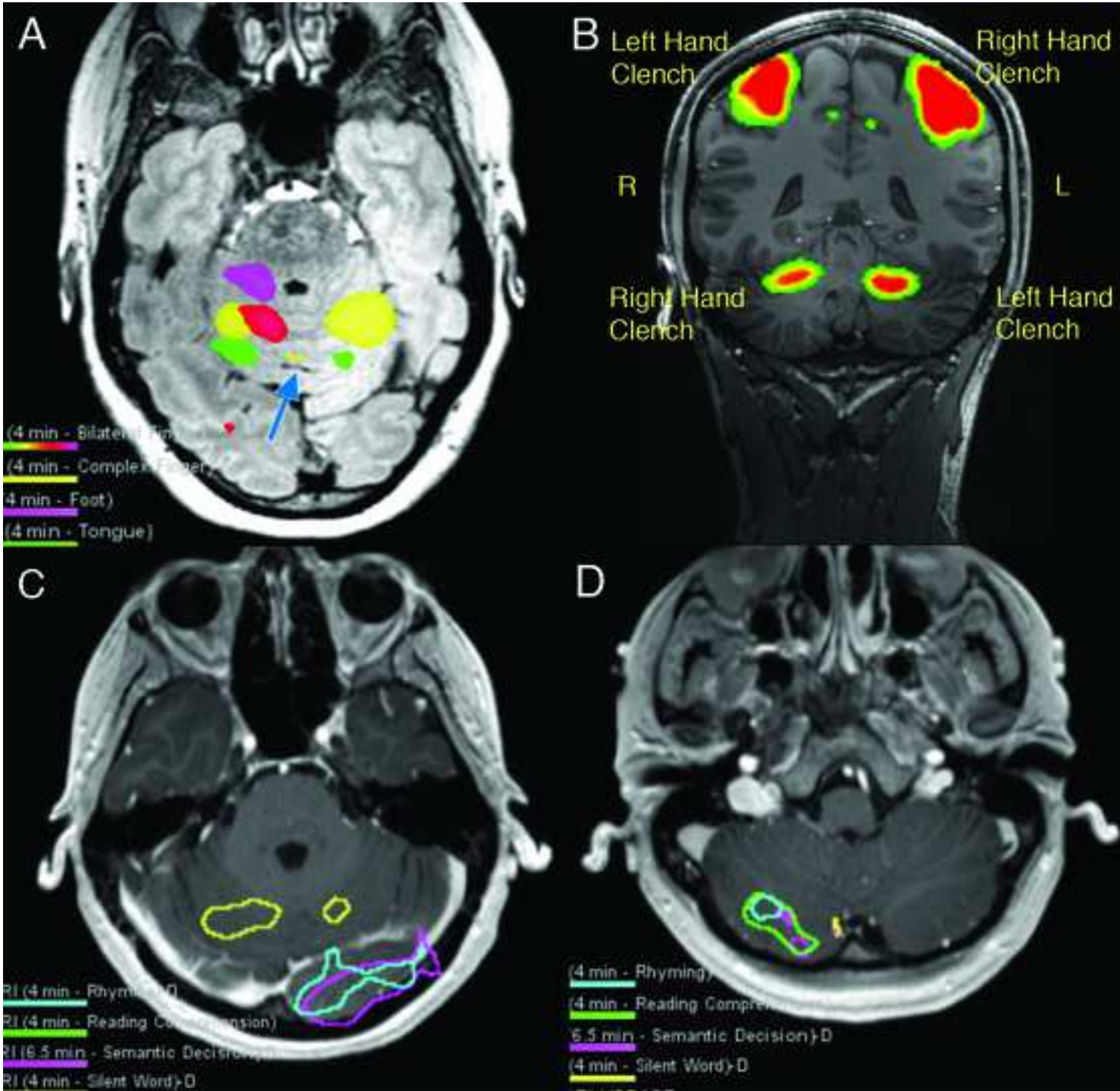
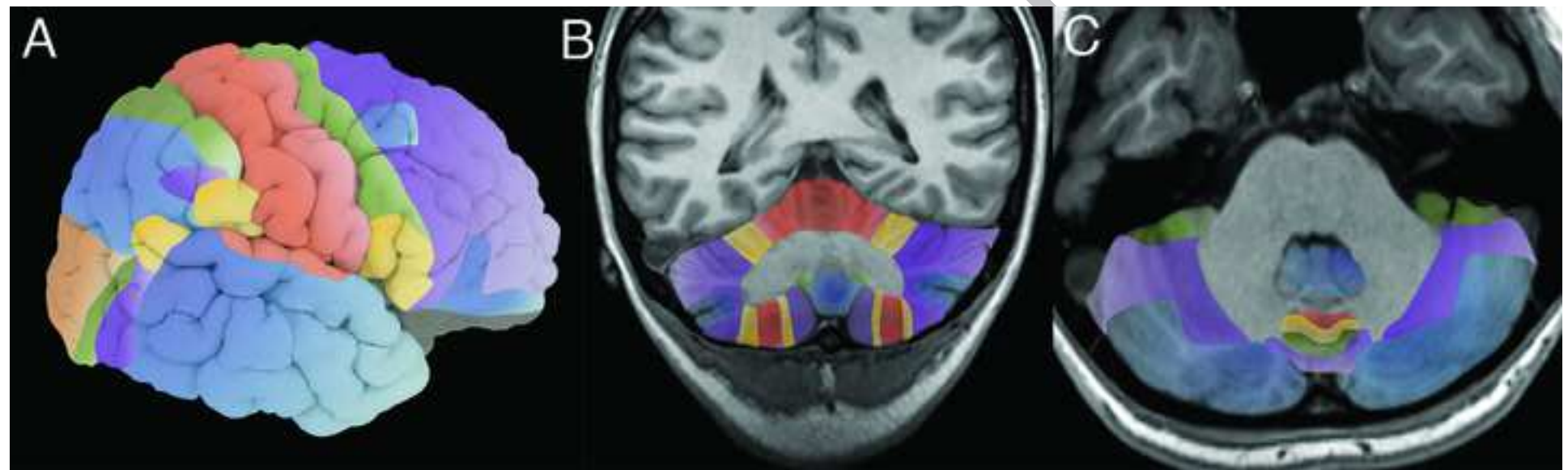
[Click here to access/download;Figure;Fig 7 new flat 300dpi CYMK.tif](#)

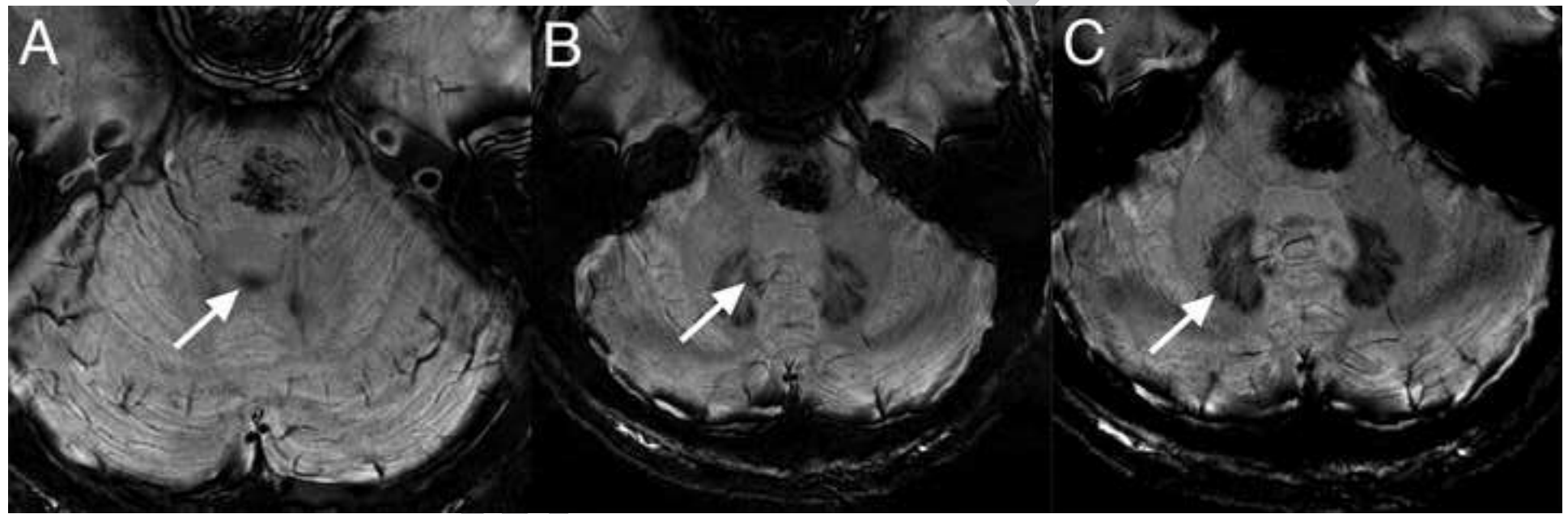
Figure 8

[Click here to access/download;Figure;Fig 8 \(old 7\) flat arrow 300dpi CYMK.tif](#)



BJR UNC

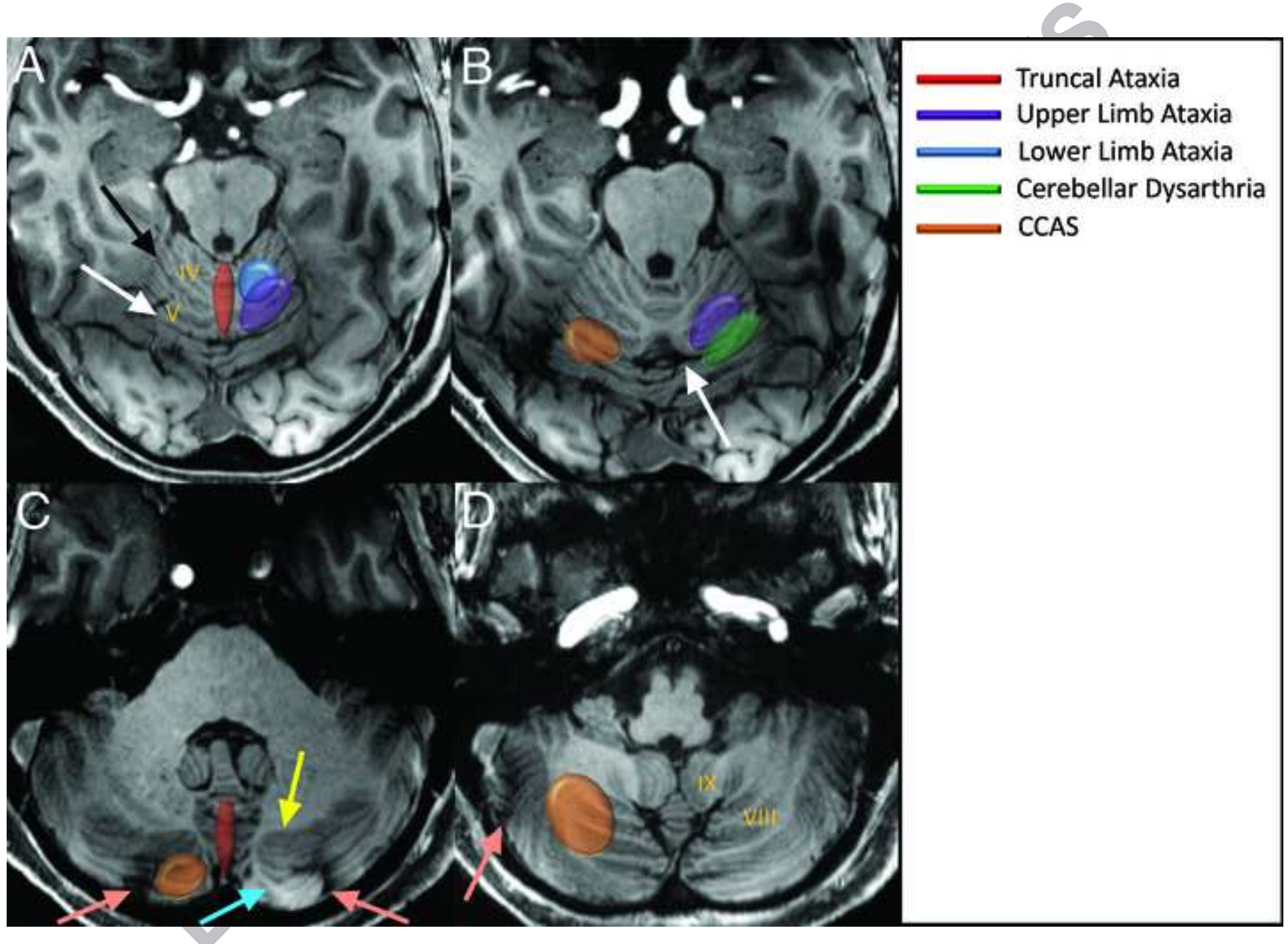
PROOFS

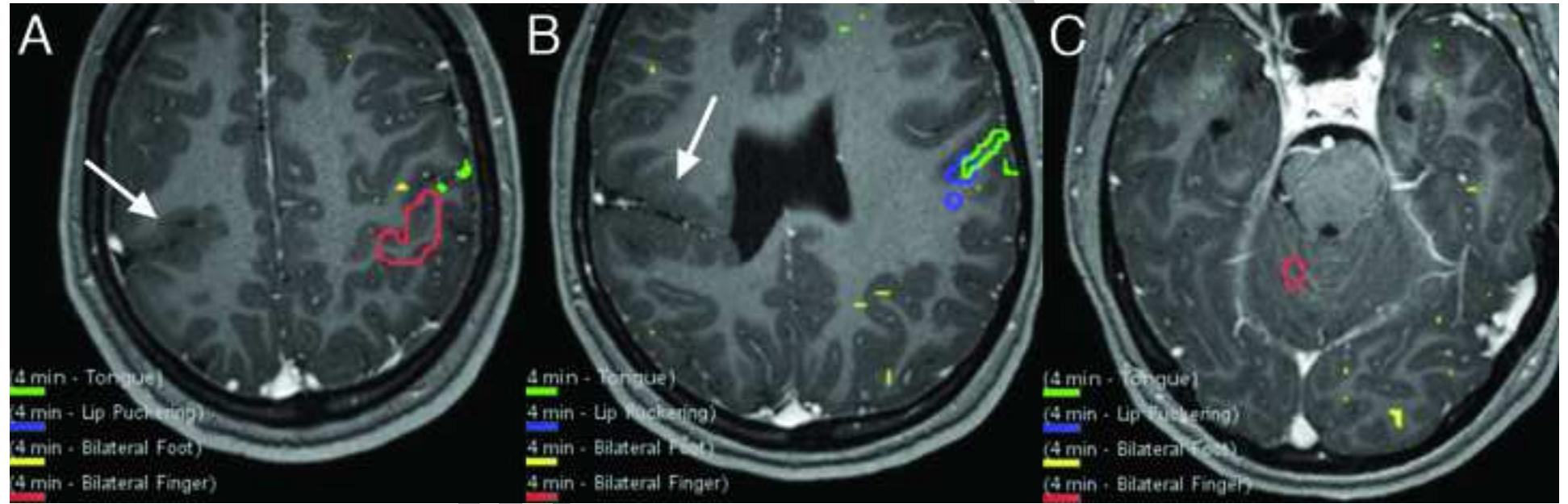


BURUNG

PROOFS

Figure 11

[Click here to access/download;Figure;Fig 11 new flat 300dpi CYMK.tif](#)



BURUNG

PROOFS

Figure 13

[Click here to access/download;Figure;Fig 13 flat 300dpi.tif](#) 

